The Origin of Time-Resolved Emission Spectra (TRES) Changes of 4-Aminophthalimide (4-AP) in SDS Micelles. The Role of the Hydrogen Bond between 4-AP and Water Present in Micelles

Andrzej Maciejewski,*,†,‡ Jacek Kubicki,§ and Krzysztof Dobek*,§

Department of Chemistry, Adam Mickiewicz University, Grunwaldzka 6, 60-780 Poznań, Poland, Centre for Ultrafast Laser Spectroscopy, Adam Mickiewicz University, Umultowska 85, 61-614 Poznań, Poland, and Department of Physics, Adam Mickiewicz University, Umultowska 85, 61-614 Poznań, Poland

Received: August 7, 2003; In Final Form: October 16, 2003

Hitherto, it has been commonly assumed that the changes observed in the time-resolved emission spectra (TRES) of the probe molecule placed in a micellar system have been a consequence of the process of solvation, related mainly to unspecific interactions. However, as follows from analysis of the shape and position of the TRES of 4-aminophthalimide (4-AP) dissolved in aqueous micellar solutions of SDS surfactant (0.15 M), the TRES changes especially in the first several tens of picoseconds cannot be explained only as a result of a nonspecific solvation process. The interpretation of the results obtained from the correlation function of spectral changes ($C(t)$) analyzed in terms of the process of solvation related to the relaxation of the environment would only be correct provided that there was only one emitting species in one excited state in a monocomponent solvent with no specific interactions. The excitation of the molecule of 4-AP leads to the intramolecular charge transfer (ICT) process, leading to a significant enhancement in the dipolar moment and the energy of the hydrogen bond formed by the carbonyl group of 4-AP (in the state S_1-ICT) and the water molecules present in the micelle. On the basis of TRES, the time-resolved area-normalized emission spectra (TRANES), and steady-state measurements, we have assigned the emission observed not only to the 4-AP in the S_1-ICT state but also to the S_1-exciplex (4-AP$\cdots$$H_2O$)*. Thanks to the increase in the hydrogen-bond energy after excitation, the equilibrium between the uncomplexed (S_1-ICT) and complexed (S_1-exciplex) forms is shifted to the advantage of the latter. The duration of the isoemissive point determines the dynamics of formation of the hydrogen bond, which can provide interesting information on the properties of water molecules in the vicinity of 4-AP. The results permit the time separation of the processes of the S_1-exciplex formation ($<$50 ps) and solvation ($\tau \cong 100$ ps) and their assignment to respective TRES changes. Similar results to those obtained for 4-AP in SDS are expected for other micellar systems and other probes containing both donor and acceptor group forming sufficiently strong hydrogen bonds with the water molecules from the micellar system.

1. Introduction

Micelles, microheterogeneous systems, have been recently a subject of study of many research groups. Relative feasibility of obtaining them, their well-defined shape, size, and critical micellar concentration (CMC), efficient solubilization of many compounds insoluble in water, significant effect on the kinetics of many photophysical processes, and the mechanism and kinetics of chemical and photochemical reactions justify their widespread use in chemistry, biology, medicine, and other disciplines.[1,2] Structural similarity of micellar systems (MS) to biological ones and, in particular, to biological membranes makes them very good model structures.[3] They are also used in investigation of detergents[4] and in medical studies. Micelles arouse special interest as complex systems,[5−11] along with inverse micelles,[5,6,12−21] cyclodextrines,[5,6,22−24] or gels,[6,25] in which water molecules probably behave as those in biological membranes and thus in a way different than those in the bulk water. Apart from the properties of water in micelles, of particular interest are their microviscosity (expressed by rotational or translational diffusion coefficients of molecules) and micropolarity of micelle fragments.[26−30]

The majority of the previous studies have been performed by steady-state and time-resolved optical spectroscopy with the use of a probe molecule. Correct description of the MS properties is conditioned by reliable determination of the probe position in the MS, which can be difficult. According to many authors, different probe molecules are located mainly in the MS headgroup region.[2a−c,31,32] However, as has been recently established, the probe molecules can be placed in the headgroup and core regions depending on their properties and size.[30a−c,31] Moreover, diffusion and dynamics partitioning of aromatic probes between the headgroup and core region can be observed following optical excitation of the probe,[30b−d,31] as a result of a significant change in its properties after excitation.

One of the probes[2,32] most often used in the study of microorganized systems is 4-aminophthalimide (4-AP)[9,14,16] and its derivatives.[33,34] Because of the emission properties, especially a strong dependence of the position of the fluorescence spectrum

* Corresponding authors. For K.D.: tel (+48) 61 8295012; fax (+48) 61 8257758; e-mail dobas@amu.edu.pl. For A.M.: tel (+48) 61 8291359; fax (+48) 61 8658008; e-mail maciejew@rovib.amu.edu.pl.

† Department of Chemistry.

‡ Centre for Ultrafast Laser Spectroscopy.

§ Department of Physics.

10.1021/jp036340z CCC: $25.00
Published on Web 11/22/2003

maximum (λ_{em}^{max}), quantum yield of fluorescence (ϕ_F), and emission lifetime (τ_F) on the environment properties, the 4-AP molecule has often been used in the study of properties (polarity and solvation processes in particular) of simple homogeneous and complex systems.[9,14,16,22,23,25,33,35−41]

When using 4-AP as a probe, it is usually assumed that the emission observed comes from the molecule in the S_1 state. This assumption implies that excitation of the 4-AP molecule leads to a change in its dipole moment from 3 D in the S_0 state (μ_{S_0}) to 6.5 D in the S_1 state (μ_{S_1}).[42] A change in the dipole moment is related to the intramolecular charge transfer (ICT) from the amino group (electron donor) onto the carbonyl group (electron acceptor) of the 4-AP molecule being on the same axis as the NH_2 group. This process induces a response of the environment, which tending to the energy stabilization of the system undergoes reorganization/relaxation and causes a stronger solvation of the 4-AP molecule. As a consequence, in homogeneous aprotic solvents, relatively strong bathochromic shifts in the steady-state fluorescence spectrum of 4-AP have been observed with increasing solvent polarity, for example, a shift of as much as 33 nm ($\sim$1700 cm^{-1}) of λ_{em}^{max} in acetonitrile (ACN) with respect to $\lambda_{em}^{max} = 425$ nm in diethyl ether.[38] The study of time-resolved emission spectra (TRES)[43] of 4-AP permitted a determination of solvation times in homogeneous solvents.[36] However, the assumption that the emission observed comes only from the S_1 state has been questioned by some authors[14,35,40,41] who pointed out the possibility of formation of S_1-exciplex (S_1-exc) by 4-AP in the S_1 state or the possibility of solvent-mediated proton transfer from the imino group to the carbonyl group in this molecule. Both of these processes can take place only in protic solvents (H_2O; alcohols, ROH), in which the excited 4-AP molecule efficiently forms hydrogen bonds with solvent molecules. Already Ware et al.[35] reported that the interactions of 4-AP with protic solvent molecules have been significantly stronger than those with molecules of aprotic solvents of close value of polarity function. The stronger interaction is manifested as a stronger bathochromic shift of fluorescence spectrum, a decrease in ϕ_F, and a shortening of τ_F, especially pronounced in water. In ACN, $\lambda_{em}^{max} = 458$ nm, $\phi_F = 0.63$, and $\tau_F = 14$ ns,[38] while in water, $\lambda_{em}^{max} = 550$ nm, $\phi_F = 0.01$, and $\tau_F = 1.2$ ns[14,38] (in both cases in aerated solutions). Samanta end Saroja,[44] similarly as Ware et al., have also found a substantial change in photophysical properties of a 4-AP derivative molecule on replacement of a protic by an aprotic solvent. They interpreted this effect as a result of formation of a hydrogen bond between the oxygen from the carbonyl group of an excited 4-AP molecule and the H−O bond of the protic solvent. Noukakis and Suppan[45] reported a strong bathochromic shift of λ_{em}^{max} in the solvents capable of forming hydrogen bonds and interpreted the effect as a result of a considerable increase in the dipole moment of the excited complex. Another interpretation of the differences in the properties of the excited 4-AP molecule in polar protic and aprotic solvents has been proposed by Harju et al.[41] and Bhattacharyya et al.[14] They suggested that the 4-AP molecule undergoes a solvent-mediated proton transfer from the imino group to the oxygen atom of the carbonyl group. Noukakis and Suppan[45] also considered the possibility of occurrence of this process, which would be responsible for an increase in the radiationless deactivation of 4-AP, a considerable reduction of ϕ_F, and shortening of τ_F. However, recently Aramendia et al.[40] and Samanta et al.[46] provided new important arguments for the interpretation suggested by Ware et al.[35] In particular, the former authors have shown that the emission (solvatochromic) properties of 4-AP in a mixture of toluene and ACN, that is, a polar aprotic solvent, are completely different than those in a mixture of toluene and ethanol (EtOH), that is, a protic solvent,[40] and indicated that the behavior of the excited molecules of 4-AP and its N-alkyl derivatives is very similar. In N-alkyl derivatives of 4-AP, the process of solvent-mediated proton transfer cannot take place.[46]

The molecules of 4-AP[9,47] and its derivatives[34,44] have been used as probes in investigation of properties of micellar systems. From comparison of the steady-state emission spectra of 4-AP dissolved in water and micelles, it is known that 4-AP in these systems is localized in the Stern layer of the micelles.[9] That is why the changes of the TRES obtained for 4-AP[9] and for coumarin C-480[8] (also localized in the headgroup region) in the micelles of SDS, CTAB, and TX-100 have been interpreted as a result of the solvation processes related first of all to a very slow dynamics of reorganization (mainly rotation) of water molecules being in the direct vicinity of the 4-AP and C-480 molecules inside the micelles.

Important data on the properties of the probe and thus on the properties of the MS can be obtained from the time-resolved emission measurements. Correct interpretation of the results requires a detailed explanation of the changes in the TRES, that is, in their shape and kinetics, and a determination of time-resolved area-normalized emission spectra (TRANES).[48,49] In the homogeneous systems in which the probe molecules are in aprotic monocomponent solvents, the changes in the emission spectrum are mainly and often exclusively due to the processes of nonspecific solvation. Taking into regard the spectral and photophysical properties of the probes hitherto used in MS, distinct anisotropy of MS properties including the anisotropy of polarity, and the fact that water (forming strong hydrogen bonds) is usually used as a solvent present as well inside the MS, the above assumption is no longer obvious. This fact should be also taken into regard when studying the properties of 4-AP in MS. To ensure that the above assumption is fulfilled, it must be shown that S_1-exc formed from the excited 4-AP molecule in protic solvents does not form in the MS and, even if it forms there, it does not emit radiation so is not directly observed in the emission spectra.

The explanation of the reasons for the exceptionally great effect of the environment on the ϕ_F and τ_F values, and above all on λ_{em}^{max}, particularly pronounced in protic solvents (especially in water), is a necessary condition for correct interpretation of the TRES results for 4-AP in MS with strongly protic water as a solvent. Although the value of μ_{S_1} after excitation increases almost twice relative to μ_{S_0}, it seems little probable that this particularly strong bathochromic shift of λ_{em}^{max} could originate exclusively from the solvation processes being a result of nonspecific interactions.

The main aim of our study was to determine the spectral and photophysical properties of the excited 4-AP molecule, its decay paths, and the species formed on its decay in micellar systems. To meet this aim, it is necessary to find out which processes are responsible for the changes in the shape and position of the TRES maximum. All of this requires spectral and photophysical studies of 4-AP in selected homogeneous solvents and in SDS micelle (M-SDS),[50] the properties of which have been relatively well recognized.

TRES measurements should provide information on spectral and photophysical properties of the probe but also on the real properties of the MS; therefore, it is desirable to perform the measurements of the fluorescence decay ($D_F(t)$) in a very wide range of emission wavelengths (λ_{em}) at a sufficiently high time resolution of the measuring system. The results obtained for

4-AP could as well be used for other probes, most of which, similar to 4-AP, comprise a donor and an acceptor group. For such molecules, a formation of the S_1-ICT state from the locally excited S_1-LE state, appearing as a direct result of the probe molecule excitation, is observed.[51] The formation of S_1-ICT is accompanied by a significant increase in the dipole moment in this state. Moreover, in the S_1-ICT state, the ability to form hydrogen bonds by these two groups (donor and acceptor type) changes relative to those of states S_0 and S_1-LE. As shown for a few molecules of this type (e.g., coumarin C102, C151, C153)[51b,d,52] and 4-AP in monocomponent protic solvents,[34,35,40] the excitation of the probe molecules leads to an increase in the energy of the hydrogen bonds formed by the acceptor group (usually carbonyl) with H−O bond of molecules of the protic solvent. The increase in the hydrogen-bond strength is accompanied by formation of S_1-exc[51b,52a−e] in the process of quenching of the S_1-ICT state by the solvent molecules (in MS usually water) in the nearest neighborhood through formation of new strong hydrogen bonds. The results presented in this work prove that the deactivation of the excited 4-AP molecule in M-SDS occurs according to this mechanism so in a more complex way than hitherto supposed,[9] which demands a different interpretation of TRES results.

2. Experimental Section

2.1. Materials. 4-AP (Aldrich) was purified by recrystallization from methanol. SDS (Sigma and Merck), ACN anhydrous (Aldrich), and dimethyl sulfoxide (DMSO) anhydrous (Aldrich) were used as received. In investigation of M-SDS, we used thoroughly purified and deionized water as a solvent. The absorption and fluorescence spectra of 4-AP after single and double recrystallization were the same. For the sake of comparison, the absorption and fluorescence spectra were also measured for 2−3 times higher and lower concentrations (c) of 4-AP, but no changes in the shape and positions of absorption and fluorescence spectra were noticed, which means that in the solutions studied and in M-SDS S_0-dimers were not formed. The solvents and solution of SDS ($c_{SDS} = 0.15$ M) in water did not contain impurities emitting radiation for excitation wavelength (λ_{exc}) equals 400 nm. The solutions studied were not deoxygenated. Typical concentrations of 4-AP were of the order of 10^{-4} M.

2.2. Experimental Setup. The absorption spectra were measured on a Jasco V-550 spectrometer. Steady-state emission measurements were made on a modernized MPF-3 spectrofluorimeter with a single photon counting system. Our system of time-correlated single photon counting (TCSPC) has been described in detail by Maciejewski et al.[53] In this work, we will just briefly mention that the emission spectrometer employed a picosecond laser system (Spectra-Physics) in the excitation pathway and a time-correlated single photon counting system in the detecting system. The laser system was composed of a picosecond Ti:sapphire laser, Tsunami (720−1000 nm, 82 MHz, 1 W, 1−2 ps), pumped by an argon ion laser, BeamLok 2060 (10 W), a pulse selector employed to decrease the excitation frequency to 4 MHz, and a generator of the second and third harmonics. The exciting beam of the vertical polarization was applied to excite the fluorescence collected at the magic angle polarization. The shape and the width of the laser pulses was controlled by an autocorrelator. For detection of fluorescence decays, we used a fast (proximity type, 6 μm) multichannel-plate photomultiplier, MCP−PMT R3809U-05 (Hamamatsu), upgraded constant fraction discriminator, CFD TC 454 (Tennelec), time to amplitude converter, TAC-TC 864 (Tennelec), and multichannel analyzer, Norland 5000 MCA. TAC worked in the reverse mode. The small grating monochromator used had the focal length 300 mm and aperture f/4.2. The full width at half-maximum (fwhm) of the instrument response function (IRF) was from 25 to 35 ps, depending on the measurements condition, and was very stable (±0.3 ps). Our TCSPC experimental setup can also work as a typical spectrofluorimeter with a laser as an excitation source, so the steady-state fluorescence spectra used in TRES analysis were collected with use of the same experimental setup as was used in time-resolved measurement. The fluorescence spectra were collected with a 1 nm step and spectral resolution of emission ($\Delta\lambda_{em}$) equal to about 9 nm, averaged from five accumulations, corrected with regard to the response of the photomultiplier and monochromator. The spectral resolution of the excitation laser beam ($\Delta\lambda_{exc}$) is less than 1 nm. The IRF was determined using the scattering method. As the scattering media, Ludox was used.

The results were analyzed by a homemade software, which allowed the use of the Levenberg−Marquardt[54] or Simplex[55] optimization algorithms. The capabilities of our system and analysis software have been described in our previous paper.[56] It allows measurements with subpicosecond accuracy; however, it was not possible in the experiments performed in this study. We could not use the reference method[57] of lifetime determination because of the lack of compounds of accurately determined picosecond lifetimes emitting and absorbing in the spectral range of our interest. The use of IRF determined by the scattering method in the fitting procedure means that changes of the width (shape) of IRF dependent on the emission wavelength, λ_{em}, are not taken into account. One of the main reasons for IRF dependence on λ_{em} is the effect of the grating monochromator,[58] and to minimize this effect, we applied a small monochromator with the focal length 300 mm.

The neglect of IRF changes depending on the emission wavelength means that the TRES obtained indirectly from wavelength-dependent decays on the basis of multiexponential fits cannot be treated quantitatively for the components of a single picosecond duration. In addition, the appearance of ultrashort components in the fit can be a result of noise in the early data.[48,59] Even if relevant reference standards were available, the accumulation time of experimental decay (at least 5000 counts in channel with maximum accumulation) in TCSPC system would be too long for 0.61 ps/channel, especially for measurements taken in the wings wavelength region of the emission spectrum. The long accumulation time follows from the long-lived fluorescence of 4-AP. Irrespective of the setting of TAC time range, the maximum number of photons detected per one second must be the same because of the photon pile-up effect. For long-lived fluorescence for 0.61 ps/channel and 1024 channels, only a part of all photons are detected by TAC; moreover, the photons from a given time range are divided among a greater number of channels. So to achieve good statistics, the accumulation time must be long, although on the other hand, the accumulation time must be as short as possible because of the zero time drift during accumulation of decay.[60] Therefore, the fluorescence decays were collected in 1024 channels with 2.44 and 12.2 ps/channel.

3. Results

3.1. Steady-State Emission Results. The spectra of absorption, fluorescence, fluorescence excitation, and quantum yields of 4-AP fluorescence were measured for 4-AP in DMSO, H_2O, and M-SDS. Thanks to the presence of the S═O group, DMSO can be treated as an approximate model of the polar fragment

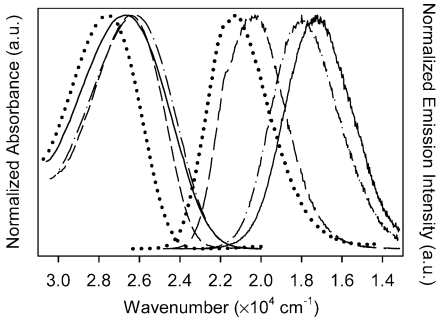

Figure 1. Normalized steady-state absorption and emission spectra of 4-AP ($c_{4-AP} \approx 10^{-4}$ M) dissolved in DMSO (− − −), ACN (···), water (—) and M-SDS (− · −) ($c_{SDS} = 0.15$ M) at $\lambda_{exc} = 370$ nm.

TABLE 1: Spectral and Photophysical Properties of 4-AP in Selected Solvents and in M-SDS ($c_{SDS} \approx 0.15$ M)

solvent	ν_{ab}^{max} [cm^{-1}]	ν_{em}^{max} [cm^{-1}]	$f(\epsilon,n)^a$	ϕ_F	τ_F [ns]	$k_F \times 10^7$ [s^{-1}]
THF	27 970	22 420	0.21	1.0[b]	20.8[b]	4.8[b]
				0.59[c]	12.4[d]	4.76
ACN	27 850	21 600	0.31	0.96[b]	14.0[d]	4.5
				0.63[c]		
DMSO	26 770	20 750	0.26	0.80	17.5	4.6
H_2O	27 100	17 700	0.32	0.01[d]	1.01	0.83
				0.01[e]	1.2[e]	
D_2O	27 150	17 570	0.32	0.045[e]	5.7[e]	0.79
M-SDS	26 600	18 200		0.067	3.2 [f]	2.09

[a] The values of ϵ and n are taken from ref 62. [b] From ref 45 in deoxygenated solutions. [c] From ref 23. [d] From ref 38. [e] From ref 14. [f] The average value of τ_{F_3}, see Table 2. Because for all wavelengths the value of τ_{F_3} is almost constant and much longer than the spectral changes, we assume that it is the average lifetime of 4-AP dissolved in M-SDS.

of the surfactant molecule with water used as a solvent. Because the positions of the maximum emission band, λ_{em}^{max}, measured earlier for 4-AP in water show significant differences (540 nm from Samanta et al.,[22,38] 556 nm from Suppan and Noukakis,[45] 550 nm from Bhattacharrya et al.[14]), we have repeated them. Figure 1 presents the steady-state absorption and emission spectra of 4-AP in water, DMSO, and M-SDS ($c_{SDS} = 0.15$ M) and for the sake of comparison in a polar aprotic solvent, ACN. The shape of the absorption spectrum, as well as emission spectrum, of 4-AP in the four systems is similar. The maximum of the long-wavelength absorption band (λ_{ab}^{max}) of 4-AP in M-SDS is the most bathochromically shifted and somewhat less in H_2O (see Table 1 and Figure 1). The differences in the positions of λ_{em}^{max} for 4-AP in the solvents mentioned above are much greater than the differences in λ_{ab}^{max}. In the case of fluorescence spectra, λ_{em}^{max} for 4-AP in H_2O is the most bathochromically shifted. The most advanced solvatochromic study performed to make a quantitative assessment of nonspecific and specific (mainly hydrogen bonds) interactions on the shape and position of the maximum of absorption and fluorescence spectra will be presented in a separate work.[61]

In this work, we are interested only in identifying the reasons for a strong effect of the solvent on the position of λ_{em}^{max} and a weaker solvent effect on λ_{ab}^{max} for the 4-AP solutions. For this purpose, we also measured the 4-AP absorption and fluorescence spectra in an anhydrous ACN, which is an aprotic solvent of a very high value of polarity function, $f(\epsilon,n)$, higher than that of DMSO and not much lower than that of H_2O (see Table 1). The fact that for 4-AP in ACN the maximum absorption and fluorescence spectrum is the most blue-shifted indicates that it is not mainly the nonspecific interactions described by the

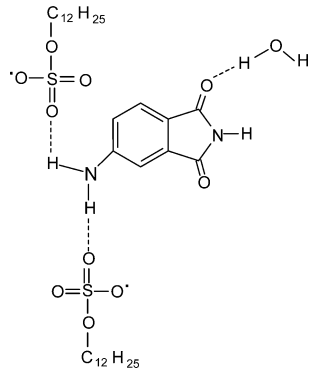

Figure 2. Structure of the 4-AP molecule with the strongest hydrogen bonds formed in M-SDS.

polarity function $f(\epsilon,n) = (\epsilon - 1)/(2\epsilon + 1) - (n^2 - 1)/(2n^2 + 1)$[62] that determine the λ_{ab}^{max} and λ_{em}^{max} and the different effects of the solvent on the absorption and fluorescence spectra. The results suggest that the interactions of the environment with 4-AP are more complex.

The 4-AP molecule can form a few hydrogen bonds with surrounding molecules of the solvent and the micellar system both of the donor type (involving the lone electron pairs on the oxygen atoms of two carbonyl groups and on nitrogen atoms of the amino and imino groups) and the acceptor type (involving three hydrogen atoms of the amino and imino groups, see the structure of 4-AP in Figure 2). A very important role of hydrogen bonds in the interactions of the excited S_1-ICT state of 4-AP molecule with the environment is directly evidenced by fact that the λ_{em}^{max} of 4-AP in water forming strong hydrogen bonds of the acceptor type ($\alpha = 1.17$)[63] is shifted by as much as 4000 cm^{-1} toward longer wavelength with respect to λ_{em}^{max} for 4-AP in ACN, which practically does not form hydrogen bonds of that type ($\alpha = 0.10$)[63] and of which the value of polarity function $f(\epsilon,n) = 0.31$ is only a little lower than that of water $f(\epsilon,n) = 0.32$. Taking into regards the results obtained for 4-AP dissolved in protic solvents[34,35,38,40] as well as for probes of similar properties,[51,52,64] this shift is interpreted mainly as a result of the hydrogen-bond formation between the oxygen atom of the carbonyl group positioned along the same axis as the NH_2 group and H−O bond of the water molecule. An important role of the hydrogen bonds formed by the hydrogen atoms of the amino group of the 4-AP molecule in the ground state is indicated by a significant bathochromic shift of the 4-AP absorption spectrum in DMSO ($\beta = 0.77$)[63] with respect to its position in the spectrum taken in ACN ($\beta = 0.47$)[63] and in H_2O ($\beta = 0.47$),[63] Table 1.

The λ_{em}^{max} of 4-AP emission recorded in water determined in our study is at 565 ± 2 nm, the authors of ref 14 report the value 550 nm, and the authors of ref 22 give 540 nm. The maximum of 4-AP emission in M-SDS is determined in this work at 549 ± 2 nm, while the authors of ref 9 give the value of ∼530 nm. The differences are significant but the values of λ_{exc} applied were also different: we used $\lambda_{exc} = 400$ nm, while in ref 9, $\lambda_{exc} = 305$ nm was used, and in ref 22, $\lambda_{exc} \geq 350$ nm was used. Differences in the spectral resolution, $\Delta\lambda_{em}$, can affect the width of the spectrum but should not cause a shift in its maximum. The spectral resolution of the spectrofluorimeters used was close to 9 nm in our system and close to 5 nm in that used in ref 9, but no data is given in ref 22.

The fact of different positions of λ_{em}^{max} obtained for 4-AP in water and M-SDS by us and in refs 9 and 22 for different excitation wavelengths could suggest a dependence of λ_{em}^{max} on the wavelength of the excitation**.** However, the results of the

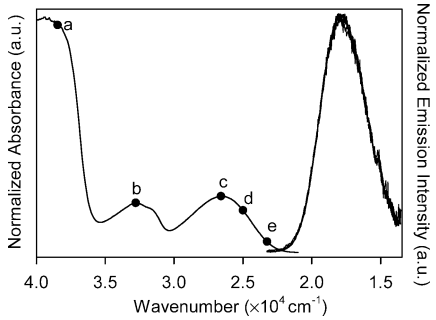

Figure 3. Normalized absorption and steady-state fluorescence spectra of 4-AP ($c_{4-AP} = 1 \times 10^{-4}$ M) in M-SDS ($c_{SDS} = 0.15$ M) obtained upon excitation at different wavelengths: 260 nm (a), 305 nm (b), 376 nm (c), 400 nm (d), and 430 nm (e).

fluorescence spectra measurements for 4-AP dissolved in M-SDS as a function of the excitation wavelength performed by us in the range $\lambda_{exc} = 260-430$ nm (Figure 3) have shown that such a dependence does not occur.[65] Moreover, no effect of λ_{em} (in the range from 480 to 650 nm) on the position and shape of the fluorescence excitation spectrum of 4-AP in M-SDS has been detected.

Quantum yields of 4-AP fluorescence on excitation in the long wavelength absorption band in M-SDS, H_2O, and DMSO were measured by a relative method using quinine sulfate in 0.1 N H_2SO_4 ($\phi_F = 0.52$) as standards.[66] The 4-AP fluorescence quantum yield was calculated from the relationship

$$\phi_F = (\phi_F)_S \frac{\int I(\nu)\, d\nu\, (I_a)_S n^2}{\int I(\nu)\, d\nu\, I_a n_S^2} \qquad (1)$$

where ϕ_F is the fluorescence quantum yield, the integral is the area under the corrected fluorescence spectrum, I_a is the absorbed intensity, n is the refractive index of the solvent, ν is wavenumbers (in cm^{-1}), and the subscript S refers to the standard in all cases. The same spectral bandwidth was used for both absorption and emission measurements.

Table 1 gives the positions of the maxima in the absorption and steady-state fluorescence spectra converted to wavenumbers (ν_{ab}^{max} and ν_{em}^{max}, respectively) for 4-AP in a few selected solvents and in M-SDS, along with the values of ϕ_F and τ_F. These data permitted a calculation of the radiative rate constants (k_F) for the emission observed from the relation $k_F = \phi_F \tau_F^{-1}$.

The values of k_F significantly depend on the properties of the environment. They are the highest (and similar) in aprotic solvents (ACN, tetrahydrofuran (THF), DMSO) and lower by over 4 times in H_2O and D_2O. The value of k_F in M-SDS is twice lower than that in the aprotic solvents and twice higher than that in water. These results strongly suggest the presence of more than one emitting species.

Not all 4-AP molecules undergo solubilization in M-SDS, some of them are still present in H_2O. However, the contribution of the 4-AP molecules present in H_2O in the experimentally determined total emission of 4-AP in M-SDS ($\lambda_{exc} = 400$ nm) was equal about 2%.[61] The concentration of 0.15 M SDS selected for the spectral and photophysical studies was chosen to ensure possibly uniform properties of the micellar system formed in these conditions by SDS,[67] the spherical shape of M-SDS,[68] and the contribution of the 4-AP molecules in the micellar systems high enough to assume that the fluorescence observed (especially in the steady-state measurements) was almost exclusively due to them.

TABLE 2: Values of the Parameters of Multiexponential Decays to Selected Fluorescence Decays, $D_F(t)$, of 4-AP ($\sim 1 \times 10^{-4}$ M) Dissolved in M-SDS (0.15 M)

time per channel [ps]	λ_{em} [nm]	τ_{F_1} [ps]	a_1	τ_{F_2} [ps]	a_2	τ_{F_3} [ps]	a_3	τ_{F_4} [ps]	a_4
2.44	480	28	0.51	210	0.12	3028	0.37		
12.2		3	0.76	249	0.08	3232	0.19	7	−0.03
2.44	555	535	0.02	1112	0.17	3448	0.81		
12.2		72	0.31	767	0.09	3113	0.90	74	−0.30
2.44	660	29	−0.36	1533	0.26	3201	1.10		
12.2		36	−0.03	1381	0.49	3128	3.61	18	−3.07

3.2. Time-Resolved Emission Spectra. The 4-AP molecule was excited with a 400 nm wavelength laser pulse in the long wavelength absorption band, $S_1(\pi,\pi^*)$. This wavelength was used to avoid possible complications of supplying too much energy, which could lead to the excitation to the state S_n ($n \geq 2$) or highly excited vibrational levels of the state S_1 ($\nu \gg 0$). Assuming that the 0−0 band is at the wavelength (~440 nm) corresponding to ~10% of the maximum of absorbance of the long wavelength absorption band, for $\lambda_{exc} = 400$ nm the vibronic excitation was estimated as ~2300 cm^{-1}. When using the $\lambda_{exc} = 305$ nm, as in ref 9, the energy excess supplied to the 4-AP molecule was high, nearly 10 000 cm^{-1}. A significant excess of energy (gained as a result of absorption of the short wavelength radiation) relative to that of the relaxed S_1 state can lead to local heating of the probe and its direct neighborhood.[69] It has been established that for coumarin 153 (C153) (it is a molecule a little greater than that of 4-AP) in monocomponent solvents, the vibrational excitation on the order of a few thousand cm^{-1} has no significant effect on the dynamics of solvation observed.[59] The excessive energy of the vibrationally excited molecule in a monocomponent solvent is released in the processes of subpicosecond intramolecular vibrational redistribution, IVR, and then effectively dissipated in the processes of picosecond vibrational relaxation by the solvent molecules.[59] In monocomponent solvents of small size molecules and small viscosity, the solvation processes are completed in single picoseconds, in water in about 1 ps.[70] When the probe molecule is inside a micelle, where the number of water molecules is not as high as that in bulk water, the process of the transfer of excessive energy to the environment (including the water molecules) can be less efficient. Therefore, the vibrational excitation can affect the results of measurements obtained for a probe in MS.

Hitherto, the TRES of 4-AP in M-SDS[9] have been interpreted as a result of solvation processes of excited 4-AP molecules through the interactions with the environment, and such an interpretation is assumed in the first part of analysis of our results. However, we point to a very important role of the time resolution of the measuring system used for the time-resolved emission spectra measurements.

The time-resolved emission spectra were obtained following the procedure of Fleming and Maroncelli.[43] The fluorescence decay, $D_F(t)$, of 4-AP dissolved in M-SDS (Figure 4) was measured for 2.44 ps/channel for λ_{em} in the range 470−690 nm and for 12.2 ps/channel for λ_{em} in the range 450−690 nm, in both cases with a step of 15 nm. The $D_F(t)$ were approximated by three- or four-exponential decays $D(t) = \sum_{i=1}^{n} a_i \exp(-t/\tau_{Fi})$. Table 2 presents exemplary values of the parameters a_i and τ_{Fi} obtained from the fit of multiexponetial decays to $D_F(t)$ for three selected λ_{em} for two chosen times per channel.

It is difficult to compare the values of decay times τ_{Fi} and amplitudes a_i for two times per channel obtained for the same λ_{em}. For 2.44 ps/channel, the correct fits were obtained for the

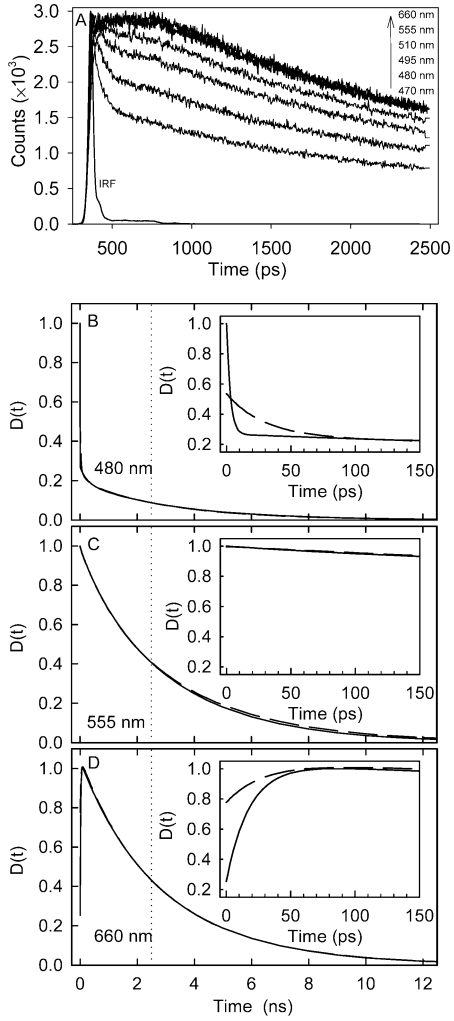

Figure 4. Experimental fluorescence decays, $D_F(t)$ (A), of 4-AP ($c_{4-AP} = 1 \times 10^{-4}$ M) dissolved in M-SDS ($c_{SDS} = 0.15$ M) at selected emission wavelengths, λ_{em}, for $\lambda_{exc} = 400$ nm and 2.44 ps/channel and kinetics of fluorescence decays, $D(t)$, determined with the use of the parameters from Table 2 (without a convolution with IRF) at 480 nm (B), 555 nm (C), and 660 nm (D) determined from the fit for 2.44 ps/channel (− − −) and 12.2 ps/channel (—).

three-exponent approximation and for 12.2 ps/channel by the four-exponent approximation. The approximation of the decay by the multiexponential function can be correct for different values of particular parameters.

Therefore, the most reliable comparison of the results given in Table 2 is obtained by the graphical method presenting the decays (without convolution with IRF) for the same λ_{em} in one graph. Figure 4B,C,D presents typical multiexponential decays obtained at the three selected emission wavelengths: in the blue range, at the maximum, and in the red range of the spectrum. The decays for the two different values of time per channel were normalized to coincide for long times (from 1 to 2 ns), for which irrespective of the time per channel they should be identical because the fwhm of IRF is ∼35 ps. No significant differences were found between the $D(t)$ obtained from the fits in the time window 12.5 ns (1024 channels × 12.2 ps/channel) and 2.5 ns (1024 channels × 2.44 ps/channel). Only for the emission decay at 555 nm, small differences were observed for long times (>2.5 ns) after excitation. It is not surprising because the emission decay determined in the time window of 2.5 ns should well describe this range of times but extrapolated to longer times it does not have to give a correct description of the decays observed in this time window. Moreover, Figure

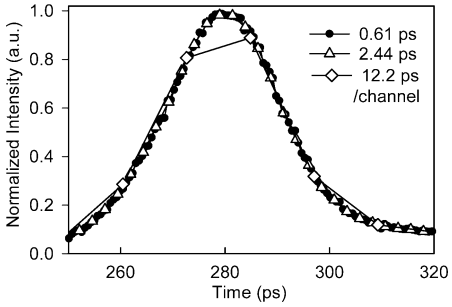

Figure 5. IRF determined for different values of time per channel. The solid lines for each time per channel value have IRF shapes taken into regard in the fitting procedure.

4B,C,D presents also the $D(t)$ in a much smaller time window (from 0 to 150 ps), in which there are significant differences between the $D(t)$ except for $\lambda_{em} = 555$ nm. The differences observed in the blue and red parts of the spectrum stem from the fact that for the measurement with 12.2 ps/channel the shape of IRF and the fluorescence decay are determined with lower accuracy for short times after excitation.

For 2.44 ps per channel, the experimentally obtained shape of IRF practically does not differ from its real shape determined for 0.61 ps/channel (see Figure 5). For 12.2 ps/channel, the distance between the subsequent experimental points increases (IRF is determined on the basis of only few points), so the shape of IRF approximated in the figure by the solid line can be increasingly different from the real IRF shape.

Therefore, to obtain accurate $D(t)$ simultaneously for long and short times after excitation, the measurements should be made with a possibly shortest time per channel but for a possibly high number of channels (e.g., 4096 channels) or two independent measurements should be made for two different times per channel and for 1024 channels.

Unfortunately, in ref 9, the authors do not give the results of the fit analogous to those given in Table 2 for 4-AP in M-SDS. A description of this important methodical aspect is usually neglected when TRES is determined. But only such results permit a direct comparison of $D(t)$ obtained by different research groups and allow analyses of possible differences in TRES.

The value of a_i amplitudes at each λ_{em} were normalized so that the area $\int_0^\infty D(t)\,dt$ was equal to the steady-state fluorescence intensity at these wavelengths. The TRES obtained were converted to wavenumbers, corrected for λ^2 and approximated by the log-normal function.[71]

Figure 6A presents an exemplary TRES and its approximation by the log-normal function for 12.2 ps/channel, and Figure 6B shows the normalized log-normal functions obtained on the basis of TRES measured for 2.44 ps/channel. The TRES determined independently for the two different time per channel values for the times starting from about 20 ps after the excitation are identical[72] and point to a distinct bathochromic shift of the emission spectra with time. However, the TRES determined for the two different times per channel for very short times after excitation, starting from $t = 0$, are significantly different. This comparison shows that because of a too small time resolution the important part of changes taking place in very short times after excitation is lost. This observation is confirmed by the time dependencies of the parameters of the log-normal function fitted to TRES presented in Figure 7: the full width at half-maximum (Γ), the intensity at the peak frequencies (h), the integrated intensity of the spectrum (I), and the asymmetry parameter (γ).[43,59] For 2.44 ps/channel, the values of these parameters change significantly in short times after excitation,

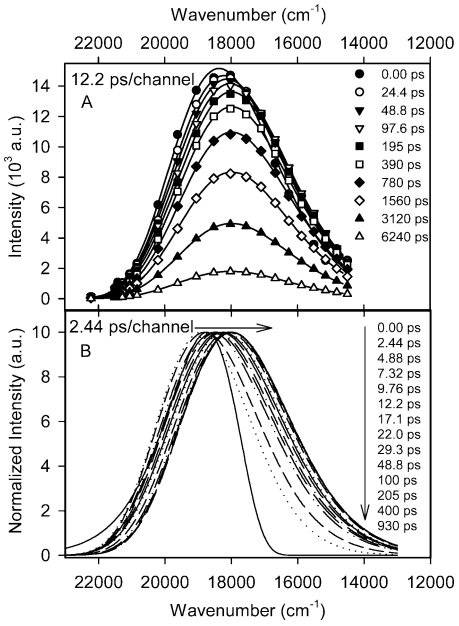

Figure 6. (A) TRES (points) and fitted log-normal curves (lines) of 4-AP ($c_{4-AP} = 1 \times 10^{-4}$ M) dissolved in M-SDS ($c_{SDS} = 0.15$ M) for 12.2 ps/channel and (B) TRES of 4-AP normalized to the same amplitude for 2.44 ps/channel.

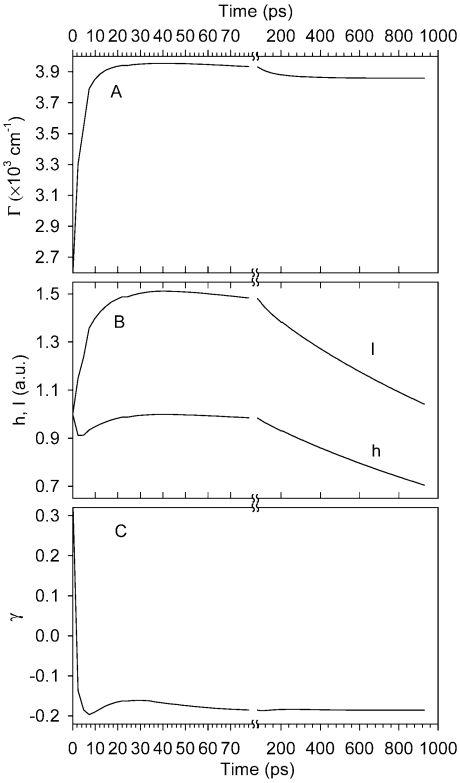

Figure 7. Parameters (Γ, full width at half-maximum; *h*, intensity at the peak frequencies; *I*, integrated intensity of the spectrum; *γ*, asymmetry parameter) of the log-normal function fitted to the TRES of 4-AP in M-SDS versus time for 2.44 ps/channel.

and starting from 40 to 50 ps after excitation, they get stabilized. For 12.2 ps/channel, the values of these parameters change in a much smaller range. Thus, the results obtained for the 2.44 ps/channel (Figures 6 and 7) strongly suggest that in short times after excitation not only the nonspecific solvation but other processes are mainly responsible for the observed spectral changes. In ref 9, the authors do not specify for which time per channel they performed the emission decay measurements for

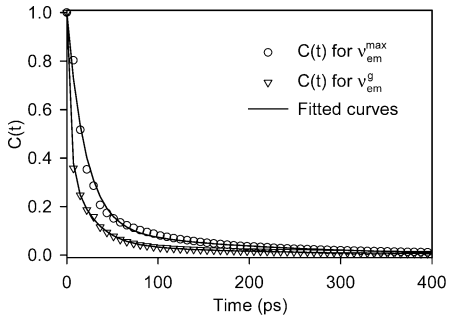

Figure 8. Correlation function $C(t)$ for ν_{em}^{max} and ν_{em}^{g} for 2.44 ps/channel.

TABLE 3: Parameters of Multiexponential Decays Fitted to *C*(*t*) Obtained for 4-AP in M-SDS

$C(t)$ from	time per channel [ps]	τ_{S_1} [ps]	b_1	τ_{S_2} [ps]	b_2	τ_{S_3} [ps]	b_3	$\langle\tau\rangle$ [ps]	$\Delta\nu_{em}^{x}$ [cm^{-1}]
ν_{em}^{g}	2.44	3	0.59	25	0.36	200	0.05	21	1665
	12.2			17	0.73	186	0.27	63	336
ν_{em}^{max}	2.44			16	0.87	146	0.13	33	927
	12.2			50	0.96	351	0.04	62	387

4-AP in M-SDS, M-CTAB, and M-TX-100. If the time of ∼82 ps that they assigned to the process of 4-AP solvation in M-SDS was to be treated as reliable, it should have been determined at a sufficiently small time per channel and for a sufficiently narrow IRF of the TCSPC system applied.

To determine the dynamics of the spectral changes observed, we resorted to the correlation function $C(t)$ for the TRES maximum (ν_{em}^{max}) and for the average (the center of gravity) wavenumber (ν_{em}^{g}), because it has been established that $C(t)$ depends on the choice of $\nu_{em}^{x}(t)$ (see eq 2).[43,73]

$$C(t) = \frac{\nu_{em}^{x}(t) - \nu_{em}^{x}(\infty)}{\nu_{em}^{x}(0) - \nu_{em}^{x}(\infty)}, \quad x \equiv \text{max or } x \equiv \text{g} \qquad (2)$$

Figure 8 presents the $C(t)$ determined on the basis of the time changes of ν_{em}^{max} and ν_{em}^{g} for the 2.44 ps/channel and its approximation by the multiexponential functions $\sum_{i=1}^{n} b_i \exp(-t/\tau_{S_i})$. Table 3 presents the decay times τ_{S_i}, amplitudes b_i of multiexponetial decays fitted to $C(t)$, the so-called mean time ($\langle\tau_S\rangle$) defined as $\langle\tau_S\rangle = (\sum_{i=1}^{n} b_i\tau_{S_i})/\sum_{i=1}^{n} b_i$, and the absolute values of the shifts of the maximum of TRES $\Delta\nu_{em}^{max} = \nu_{em}^{max}(0) - \nu_{em}^{max}(\infty)$ and the center of gravity of TRES $\Delta\nu_{em}^{g} = \nu_{em}^{g}(0) - \nu_{em}^{g}(\infty)$ obtained for 2.44 and 12.2 ps/channel. As a result of the multiexponential fit to the $C(t)$ determined on the basis of time changes of ν_g for 2.44 ps/channel, a fast component appears ($\tau_{S_1} = 3$ ps), which has not appeared as a result of the other fits presented in Table 3. In the other cases presented in Table 3, when three-exponential fits were used, two of the three τ_{S_i} parameters were equal, so we have assumed that in these cases the decays were properly described by two-exponential functions. Therefore, it has been concluded that $C(t)$ obtained on the basis of ν_g for 12.2 ps/channel and on the basis of ν_{max} for the two times per channel applied can be well described by a two-exponential decay. The values of $\langle\tau_S\rangle$ determined for 12.2 ps/channel on the basis of the time changes of ν_{em}^{g} and ν_{em}^{max} are almost identical: 63 and 62 ps, respectively. A poorer agreement between the corresponding values of $\langle\tau_S\rangle$ has been found for 2.44 ps/channel; the values were 21 and 33 ps, respectively. Moreover, for the same method of $C(t)$ determination (for ν_{em}^{g}

and ν_{em}^{max}) but for different times per channel, the parameters b_i, τ_{S_i} of the multiexponential fits, and $\langle\tau_S\rangle$ are significantly different.

Although because of the time resolution of our apparatus the real magnitude of τ_{S_i} and b_i changes can be somewhat different (especially in the first few picoseconds after excitation), the shape of the emission spectrum definitely changes.

The effect of the value of time per channel applied on the results shown in Table 3 is particularly well illustrated by the absolute values of $\Delta\nu_{em}^{x}$, x ≡ max or x ≡ g (see Table 3). For the measurements performed with 2.44 ps/channel, the differences between the values of $\Delta\nu_{em}^{x}$ for ν_{em}^{max} and ν_{em}^{g} are the greatest. For the 12.2 ps/channel, the values of $\Delta\nu_{em}^{x}$ are almost the same. This observation can be explained by the fact that for the 2.44 ps/channel the TRES for $t = 0$ is determined more accurately than for 12.2 ps/channel. The former is narrower, and its shape is different from that obtained for longer times, similarly as reported in ref 41, the authors of used equipment (streak-camera) of much higher time resolution (see Figure 2 in ref 41). Indeed, although ν_{em}^{max} for $t = 0$ is shifted by 927 cm^{-1} with respect to that for $t = \infty$, the corresponding shift of ν_{em}^{g} is by 1655 cm^{-1}! The differences are also well marked in the shape of the obtained $C(t)$, (Figure 8). Because of the changes in the shape and width of TRES in the first 10 ps after excitation (Figure 7), the $C(t)$ for ν_{em}^{g} decreases faster for short times. Consequently, a good fit to the $C(t)$ determined for ν_{em}^{g} with 2.44 ps/channel required the use of a three-exponent function. For the 12.2 ps/channel, the fit with a two-exponent function was good enough, see Table 3.

The above presented results clearly point to the fact that the parameters of the measuring equipment and the methods of measurements and results analysis have significant effect on the finally obtained values of τ_{S_i}, b_i, $\langle\tau_S\rangle$, and $\Delta\nu_{em}^{x}$.

Although the TRES results presented are complex and thus their interpretation is difficult, because they describe the dynamics of the time changes of the probe emission properties they are necessary for the correct interpretation of its properties in such complex systems as micelles. It should be noted that the dynamics of the $C(t)$ changes reflects all of the processes leading to the time changes of TRES,[74] and the clearly marked differences in the values of τ_{S_i}, b_i, and $\langle\tau_S\rangle$ obtained for ν_{em}^{g} and ν_{em}^{max} are a direct indication that the emission properties of a system studied (4-AP in M-SDS in water as a solvent) are more complex. In other words, these results provide direct evidence that in the system of 4-AP in M-SDS dissolved in water there are other processes accompanying the nonspecific solvation and that there is more than one emitting species.

The interpretation of the results obtained from the $C(t)$ analyzed in terms of the process of solvation related to the relaxation of the environment would be correct only provided that there was only one emitting species in one excited state in a monocomponent solvent with no specific interactions. If this had been true, the shape of the emission spectrum should not have changed significantly with time. In such a case, it would be justified to determine $C(t)$ for ν_{em}^{max}. As mentioned above, such a situation occurs in monocomponent solvents with no specific interactions; however, it should always be carefully verified in micellar systems. For the micellar systems and other microorganized systems, it is necessary to identify the real reasons for the time changes of the spectra, which requires a determination of TRANES for a system studied.

3.3. Time-Resolved Area-Normalized Emission Spectra. The method of the TRES spectra normalization with respect to the area under the spectral curve for $t = 0$ can be used to find out whether there are only one or two or more species emitting in the wavelength range considered. The conclusion of the presence of more than one emitting species is drawn on the basis of the appearance of the isoemissive points in the normalized spectra. The method has been used for the micellar studies by Pansu et al.[31] It has been called TRANES and used by Periasamy et al.,[48,49] in investigation of organized molecular assemblies and solvent mixtures. According to refs 48 and 49, one isoemissive point can occur in the two following situations. First, if there is only one species in the ground state A, after excitation we observe the emission from the excited species A* and the emission of the excited species B* formed directly from A*. Second, if there are two species A and B already in the ground state, then upon excitation we observe the emission from the two excited species, and both A and B or A* and B* or both can be kinetically coupled. The two species in the ground state can also be the same chemical species but in two different environments in the organized molecular assemblies. As follows from the data reported by the same authors, the process of solvation (many species with continuum distribution of energy level and continuum distribution of emission spectra) will disturb the detection of the isoemissive point. Taking into account the properties of the probes (including 4-AP), their site distribution in the polar fragments of the micellar systems studied, and the presence of water molecules in the neighborhood of the probe molecules, it is reasonable to assume the occurrence of the solvation processes. If the solvation processes are much slower or much faster than the rate of formation of B* from A* (in the first situation) or than the rate of reaching a new equilibrium between A* and B* (in the second situation), it will be also possible to observe an isoemissive point. If the solvation processes take place in the same time range as the above-mentioned two processes and are accompanied by considerable spectral changes, the isoemissive point may be unobserved. Figure 9 presents TRANES of 4-AP in M-SDS for 2.44 ps/channel. The spectra shown are the log-normal curves fitted to the experimental spectra and then normalized to the same area under the curve. By using such log-normal curves, one assumes that the emission spectra of all emitting species in the system give a mean spectrum that is well described by a single log-normal function. However, this assumption was justified thanks to a good quality of the fit of single log-normal functions to measured TRES. Both in the experimentally obtained TRANES and the log-normal approximations, the isoemissive point appears at $\lambda \approx 552$ nm ($\nu = 18\,120$ cm^{-1}) at the time from 10 to about 50 psafter excitation. Figure 10 presents a normalized

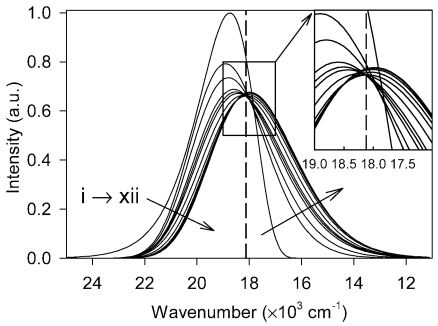

Figure 9. TRANES of 4-AP ($c_{4-AP} = 1 \times 10^{-4}$ M) in M-SDS ($c_{SDS} = 0.15$ M) generated from fitted log-normal curves for 2.44 ps/channel: (i) 0.00, (ii) 2.44, (iii) 4.88, (iv) 7.32, (v) 9.76, (vi) 12.2, (vii) 24.4, (viii) 48.8, (ix) 100, (x) 200, (xi) 400, and (xii) 800 ps. Dashed line represents the wavenumber at which the isoemissive point appears.

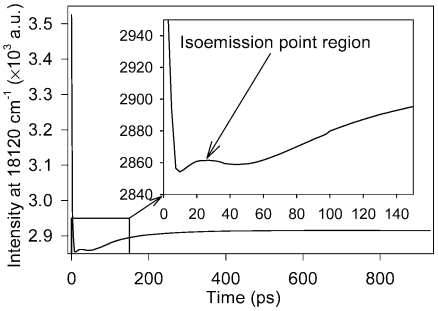

Figure 10. The normalized intensity of emission at 18 120 cm^{-1}, see Figure 9.

intensity of emission at 18 120 cm^{-1} from Figure 9, corresponding to the wavelength at which the isoemissive point is observed. About of 50 ps after excitation, the normalized intensity of the spectra for $\lambda = 552$ nm ($\nu = 18\,120$ cm^{-1}) begins to exponentially increase with the time $\tau_N = 101$ ps.

4. Discussion

4.1. Spectral and Photophysical Results. At first we shall concentrate on trying to establish the real reasons for the emission changes observed for different times of delay (TRES) for 4-AP in M-SDS and to identify the species present in the system before and after the excitation of 4-AP molecules in M-SDS, referring to the hitherto published results of spectral and photophysical properties of 4-AP and relevant results of this work. A particularly interesting property of 4-AP is a very strong dependence of λ_{em}^{max} on the solvent properties. As follows from the solvatochromic measurements in chloroalkanes ($\alpha = 0$, $\beta = 0$)[63] but also in aprotic solvents (including ACN), there is a linear dependence between λ_{em}^{max} and the value of the solvent polarity function, $f(\epsilon,n)$.[61] In the solvents capable of forming hydrogen bonds, either donor or acceptor type, significantly stronger than ACN, an additional bathochromic shift $\Delta\nu_{em}^{shift}$(H-bond) of steady-state fluorescence spectrum is observed. It is particularly great in water, 5300 cm^{-1}, and in M-SDS, 4900 cm^{-1}.[75] As indicated by many results, including neutron diffraction[76] and NMR[77] and EPR[68,78] studies, water used as a solvent is also present in M-SDS, especially close to the headgroups and a few methylene groups from the dodecyl chain bonded through the oxygen atom to the headgroups.[68,77b,79] The argument indicating that formation of hydrogen bonds has significantly greater effect on the long wavelength position of steady-state fluorescence spectra than the nonspecific (particularly dipole−dipole) interactions is provided by a comparison of the position of λ_{em}^{max} in *tert*-butyl alcohol (*t*-BuOH) and ACN. Despite a greater value of the polarity function $f(\epsilon,n)$ for ACN ($f(\epsilon,n) = 0.31$) than for *t*-BuOH ($f(\epsilon,n) = 0.25$), the maximum of steady-state fluorescence spectrum in this alcohol is bathochromically shifted by as much as 1800 cm^{-1} relative to its position in ACN.[38] Very similar results have been obtained for 4-AP in binary solvents being mixtures of toluene with EtOH or with ACN.[40] In the spectrum recorded for 4-AP in the mixture with EtOH, being a protic solvent capable of hydrogen-bond formation, a very strong bathochromic shift of steady-state fluorescence spectrum was observed even in the presence of small amounts of this solvent (see Figure 3 in ref 40) by $\Delta\nu_{em}^{shift}$(H-bond) = 2700 cm^{-1} for ∼1.5% EtOH and $\Delta\nu_{em}^{shift}$(H-bond) = 3800 cm^{-1} for 5% EtOH, which makes ∼60% and ∼83% of the total spectral shift between toluene and EtOH, equal to 4600 cm^{-1}. In the spectrum recorded for 4-AP in the mixture of toluene and ACN in the same relative concentrations as EtOH in the above mixture, the bathochromic shift was 300 cm^{-1} for 1.5% ACN and 650 cm^{-1} for 5% ACN, which makes 15% and 32% of the total spectral shift (equal to 2000 cm^{-1}) of the maximum of steady-state fluorescence spectrum for toluene and ACN. A comparison of these results clearly indicates that despite similar values of $f(\epsilon,n)$ for EtOH and ACN, the bathochromic shift of the steady-state fluorescence spectrum in the mixture of toluene−EtOH was 9 times greater than that in the mixture of toluene−ACN for the same concentration (1.5%) of the polar component. The results presented above, along with those obtained for different concentrations of EtOH and ACN in toluene, clearly illustrate a completely different behavior of the excited 4-AP molecule in the S_1-ICT state if in the first solvation sphere there is a protic solvent molecule capable of forming hydrogen bonds with 4-AP (between the carbonyl group of the 4-AP molecule and the H−O bond of the solvent molecule), for example, EtOH.

In contrast to the steady-state fluorescence spectrum, the effect of aprotic solvents on the position of the absorption spectrum maximum is relatively small. The maximum of the absorption spectrum is bathochromically shifted with increasing $f(\epsilon,n)$ of the solvent, but the shift is over 2.5 times smaller than that of the steady-state fluorescence spectra.[61] The absorption spectrum maximum of 4-AP in solvents capable of forming hydrogen bonds shows a small bathochromic shift relative to that in the aprotic solvents of the same value of $f(\epsilon,n)$, for example, in water by 1400 cm^{-1} [61] (like in MeOH[61]), almost 6 times smaller than the shift of the maximum in the steady-state fluorescence spectra. This fact means that although the 4-AP molecule forms hydrogen bonds in the ground state, they are much weaker than those in the S_1-ICT state, from which fluorescence is emitted. This difference illustrates considerable differences between the 4-AP molecule properties in the LE state (observed in the absorption spectra) and in the ICT state observed in the steady-state fluorescence spectra. The longest wavelength position of the absorption spectrum maximum in monocomponent solvents ($\lambda_{ab}^{max} = 374$ nm) has been observed in DMSO forming only donor hydrogen bonds ($\beta = 0.77$) with the H−N bonds of the amino and imino groups of the 4-AP molecule. Formation of these hydrogen bonds is responsible for a bathochromic shift of the absorption spectrum, for example, in DMSO by as much as ∼2000 cm^{-1}, relative to that of another solvent of the same value of polarity function $f(\epsilon,n)$ but in which no hydrogen bonds are formed.[61] A similar bathochromic spectral shift caused by the hydrogen bonds has been observed of the maximum of the steady-state fluorescence spectrum of 4-AP in DMSO (by ∼2400 cm^{-1}). The most bathochromic position of the maximum of the absorption spectrum ($\lambda_{ab}^{max} = 378$ nm) of 4-AP in M-SDS of all of the systems studied is a consequence of formation of hydrogen bonds between the H−N bonds of the amino group and the oxygen from the O−SO_3^- group of the surfactant molecules forming M-SDS (analogously as in DMSO) and between the oxygen atom of the carbonyl group placed at the same axis as the amino group and the H−O bonds in water molecules (of $\alpha = 1.16$) present in M-SDS.

The results of the emission study have shown that if there is a molecule of a protic solvent near an excited 4-AP molecule, they will form a strong hydrogen bond of energy much higher than average thermal energy of each molecule ($k_BT \approx 210$ cm^{-1} at room temperature). According to the model proposed by Ware at al.,[35] this hydrogen bond formation leads to the efficient formation of S_1-exc. A very similar behavior to that of 4-AP in the presence of aprotic and protic solvents has been established

for 4-AP derivatives, especially for those in which hydrogen in the imino group has been replaced by the methyl group[61,80] or other substituents.[38,40,44,46,80,81] In the molecules of such derivatives, the process of solvent-mediated proton transfer from the imino group to the carbonyl group, involving a protic solvent and leading to keto−enol tautomery, postulated for the 4-AP,[14,41] is impossible.

The process of solvent-mediated proton transfer involving amino protons of 4-AP through two water molecules into the carbonyl group[82] can be also excluded as responsible for the very strong bathochromic shift emission spectrum observed for 4-AP in M-SDS, significant decrease in Φ_F and τ_F relative to the corresponding values for 4-AP in polar but aprotic solvent. This conclusion is based on the fact that the $\Delta\nu_{ab}^{shift}$(H-bond)[83] value is significantly greater in aprotic DMSO ($\beta = 0.77$) than in H_2O ($\beta = 0.47$). Taking into regard the same properties of the S═O bonds in the OSO_3 group in the SDS surfactant molecule (forming a micelle) and in the DMSO molecule, one can assume that this bond will form a hydrogen bond with the N−H bonds of amino goup of 4-AP in S_0 state.

The presence of more than one emitting species in the system of 4-AP in M-SDS is clearly indicated by the results of photophysical studies. The values of k_F determined for 4-AP in the S_1-ICT state determined on the basis of the accurately measured values of ϕ_F and τ_F are 4 times smaller in H_2O and D_2O than in aprotic polar solvents (e.g., ACN) and about twice smaller than in M-SDS (Table 1). Very similar results of solvatochromic measurements, ϕ_F and τ_F have been obtained for aminonaphthalimide derivatives in EtOH containing unsubstituted NH and NR groups.[80,81] The presence of two emitting species, the 4-AP molecule in the S_1-ICT state and S_1-exc, is evidenced by a significant effect of the solvent deuteration on values of ϕ_F and τ_F, $\phi_F(D_2O)/\phi_F(H_2O) = 4.5$ and $\tau_F(D_2O)/\tau_F(H_2O) = 5.7$.[14] It should be noted that similar results have been obtained for 4-AP and N-methyl[61] and N-alkyl derivatives of 4-AP;[46] in the latter molecules the process of proton transfer from N−H onto C═O is not possible.

It should be emphasized that the presence of the amino group has a considerable effect on the emission properties of 4-AP and its derivatives. The study of emission properties of phthalimides and related compounds (i.e., the molecules differing from 4-AP and its derivatives by the lack of amino group) in solvents forming both donor and acceptor hydrogen bonds (including water) has shown that the position of the maximum of steady-state fluorescence spectrum of phthalimides and related compounds is very similar in different solvents. It lies at much shorter wavelength (by over 6000 cm^{-1}) with respect to that of 4-AP in H_2O, and it is almost the same as that for 4-AP in nonpolar solvents (in aliphatic and aromatic hydrocarbons).[62] Thus, it is clearly indicated by the results of solvatochromic study ($\Delta\nu_{em}^{shift}$(H-bond) and $\Delta\nu_{ab}^{shift}$(H-bond)[83]) and photophysical study (k_F, $\phi_F(D_2O)/\phi_F(H_2O)$, $\tau_F(D_2O)/\tau_F(H_2O)$) that in protic solvents (ROH, H_2O, D_2O) there are two emitting species and not one. However, the shape of the steady-state fluorescence spectrum of 4-AP in M-SDS is constant, irrespective of λ_{exc} in the range from 270 to 430 nm, and the quantum yield of fluorescence is practically the same under a long wavelength excitation ($\lambda_{exc} = 430$ nm), $\phi_F = 0.064$, and under excitation at the maximum of the $S_0 \rightarrow S_1$ absorption band ($\lambda_{exc} = 380$ nm), $\phi_F = 0.067$. Moreover, the fluorescence excitation spectrum has the same shape in the whole range of emission studied. This means that both species (the 4-AP molecule in the S_1-ICT state and S_1-exc) are at equilibrium. Taking into regard the fact that their lifetime in M-SDS is of a few nanoseconds, this conclusion seems fully justified. It is worth noting that the presence of two emitting species, the molecule of 4-AP in the S_1-ICT state and S_1-exc, formed as a result of this excited-state quenching by molecules containing an H−O bond (ROH, H_2O, D_2O) has been observed for 4-AP in monocomponent (homogeneous) and binary solvents containing protic component.[35,40,45] The driving force of S_1-exc formation in M-SDS is the formation of a strong hydrogen bond between the oxygen of the carbonyl group of relatively high electron density in the S_1-ICT state and the H−O bond of water molecules. High energy of the hydrogen bond is confirmed by a bathochromic shift of the steady-state fluorescence spectrum maximum by about 3700 cm^{-1} for 4-AP in M-SDS[61] relative to that of 4-AP in ACN, having a similar value of $f(\epsilon,n)$ but incapable of forming hydrogen bonds.[84]

4.2. TRES Results. Interesting, although in view of the results of ref 9, unexpected, are the results of the time-resolved emission measurements. Directly after excitation, the shape of the TRES spectrum is distinctly changed (Figure 6B), and its width considerably changes in short times after excitation (Figure 7A). The changes in TRES are much more pronounced in the time 0−20 ps after excitation than later. Moreover, between 10 and 50 ps, the TRANES reveals a clear isoemissive point (Figures 9 and 10).

All of the results of time-resolved emission measurements, together with the solvatochromic data for 4-AP in solvents capable of hydrogen-bond formation (both protic and aprotic) and the clearly observed dependence of k_F on the solvent used, show that for 4-AP in M-SDS the emission originates from more than one species. The hitherto TRES results for 4-AP in M-SDS[9] and in other MS[9] and for other probes (especially coumarins) in MS have been explained assuming that the spectral changes are due to nonspecific solvation. Therefore the results obtained in this study will be initially interpreted under the same assumption to show that it leads to erroneous results. We also want to illustrate the effect of the parameters of the experimental setup (not only fwhm of IRF but also the value of time per channel) on the final data. Taking into account the above-described changes of the TRES shape, the analysis of TRES results is based on the values of $C(t)$ obtained for ν_{em}^{g}.[73] A preliminary analysis of TRES and $C(t)$ obtained for 12.2 ps/channel can lead to results qualitatively similar to those published in ref 9. However, to get a good approximation of $C(t)$, we had to use two- or three-exponential functions depending on the time per channel value used and on whether $C(t)$ was determined for ν_{em}^{max} or ν_{em}^{g}, while in ref 9, the authors describe the $C(t)$ decay by a monoexponential function ($\tau_{S_1} =$ 82 ps) and for ν_{em}^{max}. To be more exact, they described the fluorescence decay in the blue range by a monoexponential function and in the red range by a two-exponential function. It must also be emphasized that they applied a global analysis. The approximation of our fluorescence decays in the blue range by a monoexponential function was unacceptable; we had to use a three-exponential approximation, and in the red range, we even had to use a four-exponential fit (see Table 2). Also the values of $\Delta\nu_{em}^{g} = \nu_{em}^{g}(0) - \nu_{em}^{g}(\infty)$[73] obtained by us differed from those given in ref 9, see Table 3 in this paper and Table 1 in ref 9. The differences are explained at least in part by differences in the shape of the steady-state fluorescence spectra, manifested as a difference in the positions of their maxima. Another source of the differences can be different time resolutions of the measuring systems (25−35 ps of our system and ∼50 ps the system used in ref 9) and different values of time per channel. The application of a monoexponential function

to approximate the $C(t)$ course obtained in our study gave a much poorer fit than that by two- and three-exponential functions. In the case of a monoexponential function, τ_{S_1} obtained by us was still different from that given in ref 9 and was equal to about 15 ps. The attempts at a monoexponential fit to $C(t)$ gave $\tau \approx 100$ ps, a similar value to that obtained in ref 9 but for the time range from 50 ps after excitation, so for the time when fast changes in the shape of TRES stop. Although this fit in this time range of $C(t)$ was better than that by a monoexponential function in the whole time range, it was not correct. A monoexponential approximation of a satisfactory fit quality was obtained for the time range from $t \approx 100$ ps after excitation. However, for this time range, we obtained about 190 ps so the same value as τ_{S_3} for 2.44 ps/channel and for ν^{g}_{em} (see Table 3). This result is consistent with expectations, because starting from 100 ps after excitation the contribution of the two shorter components ($\tau_{S_1} = 3$ ps and $\tau_{S_2} = 25$ ps, see Table 3, 2.44ps/channel, ν^{g}_{em}) describing the kinetics of $C(t)$ is insignificant. Nevertheless this contribution is significant for the first 100 ps. The fastest component, τ_{S_1}, obtained for 2.44 ps/channel could be related to solvation of unbound water molecules behaving similarly to bulk water. It cannot be excluded that distinct changes observed directly after excitation in the short wavelength range (Figure 6B) are a result of deactivation of the 4-AP from the state S_1-LE to the state S_1-ICT, which is related to a significant change in the electron density distribution as a result of the 4-AP excitation, that is, an increase in the electron density on the oxygen atom of the carbonyl group. However, taking into regard the fact that in the fitting procedure for all λ_{em} the same IRF was used, (see section 2.2, Experimental Setup), the value of this fast component must be treated with caution. It should be noted that the time τ_{S_1} corresponds to the time per channel of 2.44 ps/channel. Of course, it is difficult to estimate a direct relation between the time resolution of fluorescence decay measurement and the time resolution of the correlation function $C(t)$ obtained. It should also be remembered that the fits to the fluorescence decays for short times can be charged with errors following from the method of determination of the IRF. Consequently, TRES in short times can be also charged with some error. The dynamics of $C(t)$ changes is directly related to the change of the weighted frequency position ν^{g}_{em}. The fast component τ_{S_1} of $C(t)$ is thus related to the fast changes in the position of ν^{g}_{em}. Interpretation of the component τ_{S_2} thus requires taking into account the spectral and photophysical results obtained for 4-AP and the presence of the isoemissive point in TRANES (Figure 9). The results of TRANES show that the time, $\sim\tau_{S_2}$, does not describe the process of solvation but rather the process of quenching of 4-AP in the S_1-ICT state by the closest water molecule and formation of the emitting S_1-exc. The TRES spectra for $t > 50$ ps after excitation (when the isoemissive point disappears) practically do not change the shape and width but reveal a small bathochromic shift with time. Taking into account the fact that the TRES are a result of the emission of S_1-ICT and S_1-exc, it can be assumed that the long-time component, τ_{S_3}, is related to the process of solvation of both these species. Although a quantitative discussion of the results is not the aim of this study, taking into account the position of the fluorescence spectra of these two species it can be expected that the spectral changes of TRES in the short wavelength range are determined mainly by the process of solvation of S_1-ICT and in the long wavelength range mainly by the process of solvation of S_1-exc. One also has to bear in mind that the nonspecific solvation of both species can occur with different relaxation times and can lead to different $\Delta\nu^{x}_{em}$ (x $\equiv$ max or g) values. As a result, the $C(t)$ changes observed in the time range in which the TRES width does not change significantly ($t > 100$ ps) should be considered as the resultant bathochromic shift of the S_1-ICT and S_1-exc spectra (spectrally separated) due to nonspecific solvation and to the process of S_1-exc formation, which in this time range can be neglected.

4.3. TRANES Results. The changes in the shape of TRES particularly great in short times after excitation (Figure 7) suggest the presence of more than one emitting species in the system. To confirm this conclusion, an analysis of the TRANES spectra was undertaken. For a short time from about 10 to ~50 ps after excitation, the time-resolved area-normalized emission spectra show a slightly broadened isoemissive point (Figures 9 and 10). As has been shown in refs 31, 48, and 49, the presence of one isoemission point in TRANES implies the presence of two emitting species in the system. This observation means that the 4-AP molecules emitting at the short wavelength range transform into another species emitting at the long wavelength range. Assuming the exponential character of this process, we can estimate its relaxation time as ~17 ps. On the basis of our results and the recent reports,[40] we found it reasonable to conclude that emitting species are the excited 4-AP molecules in the state S_1-ICT and the excited complex/S_1-exciplex (4-AP:H_2O) formed through a strong hydrogen bond.[34,35,45] In bulk water, because of a direct contact with water molecules, an equilibrium between the complexed and uncomplexed molecules is probably reached immediately after excitation (in subpicoseconds or single picoseconds). The TRES measurements performed for 4-AP in bulk water did not reveal any shift in the time detectable by our equipment, which confirms this hypothesis. In the micellar systems, there are significantly fewer water molecules than in bulk water (~11 water molecules per 1 surfactant molecule in a solution of 0.01 M SDS and ~6 water molecules per 1 surfactant molecule in a solution of 0.5 M SDS[78]). The environment in MS is also more viscous, which significantly affects the rate of translational and rotational diffusion of water molecules.[77b,85] Therefore, we can expect a much slower dynamics of S_1-exc formation in M-SDS. The results presented in Figures 9 and 10 seem to confirm the above suppositions. It should be noted that 4-AP is partly complexed already in the ground state, as indicated by the value of ν^{max}_{em} for TRES for 0 ps determined for 2.44 ps/channel. The TRES for $t = 0$ ps is significantly (by ~1400 cm^{-1}) shifted toward long wavelength relative to steady-state fluorescence spectrum measured in DMSO, a solvent of similar value of $f(\epsilon,n)$ to that of water but being aprotic. The complex emits immediately after excitation in a longer wavelength range than uncomplexed 4-AP. However, a significant number of 4-AP molecules do not form complexes with water at that time yet. After excitation of the uncomplexed molecules, they are also emitting, but the ratio of the complexed and uncomplexed molecules changes. The number of the complexed molecules increases because the electron density transition from the amino to the carbonyl group significantly increases the acceptor properties of the C═O group, enhancing the energy of the hydrogen bond of 4-AP in S_1-ICT relative to that with 4-AP in S_0 with H−O from water. As suggested by the observations of Gustavsson et al.[86] the presence of different electronic states of an excited molecule (e.g., coumarin 151) can be also responsible for the dynamic Stokes shift. For example, a transition from the locally excited state to the charge transfer state or a relaxation from highly excited vibronic states to a relaxed vibronic state can lead to a dynamic Stokes shift. We expect that the transition

from the S_1-LE state to S_1-ICT of 4-AP occurs in a very short time after excitation, similarly as in coumarin 151, because of similar size of these molecules and also because of other similar properties. Therefore, excited states other than S_1-ICT cannot be responsible for the picosecond emission observed for 4-AP in M-SDS. Because the isoemissive point disappears after ~50 ps, it is reasonable to assume that in the micellar environment an equilibrium between 4-AP in the state S_1-ICT and S_1-exc is reached in this short time. Both of these species have the same lifetime ($\tau \approx 3.2$ ns) because they are kinetically strongly coupled and undergo solvation, which may have, as has been mentioned in the precedent section, different dynamics for each of them. The exponential increase with the time $\tau_N = 101$ ps of the normalized intensity for 18 120 cm^{-1} after 50 ps, when the isoemission point ceases to be seen (Figure 10), cannot be in a simple way related to analysis of $C(t)$. The parameter τ_{S_3} has been determined from the fit of multiexponetial decays to $C(t)$ in the whole time range as the longest exponential component and the parameter τ_N from the fit to normalized intensity of emission at 18 120 cm^{-1} (for the isoemissive point) as a result of one-exponential fit started from $t = 50$ ps after excitation. The value of τ_N is consistent with the result of the fit of a monoexponential decay ($\tau = 100$ ps) to $C(t)$ in the same time range, that is, for the times longer than 50 ps. After this time, the spectrum shape changes stop (an equilibrium is reached between the complexed and uncomplexed species), and as we suppose, then further changes of $\nu^g_{em}(t)$ are related mainly to the processes of nonspecific solvation. Thus, the correct mean value of the relaxation time of the solvation is close to 100 ps, similar to that obtained in ref 9, however, obtained in a completely different way.

In view of the results of TRANES, new interpretations of the times τ_{S_1} and τ_{S_2} appear. The excitation of the ground-state complex 4-AP:H_2O must lead to the charge-transfer process from amino to carbonyl group (similarly as in 4-AP molecule), which through an increase in the electron density on the oxygen atom causes an increase of the energy of the hydrogen bond forming the complex. The increase in the hydrogen-bond energy is accompanied by a shortening of its mean length. These processes take place in a certain finite time and lead to an energetic stabilization of the complex, which is responsible for the bathochromic shift in the emission spectrum of the complex. The shortest time, τ_{S_1}, can be related to these processes. The time τ_{S_2} can be related to the process of reaching a concentration equilibrium between the 4-AP in S_1-ICT state and S_1-exc. Having in mind the presence of two emitting species and the time resolution of our equipment, we cannot treate the interpretation of the times, especially τ_{S_1}, quantitatively. Moreover, the process of reaching a new equilibrium after excitation does not have to be described by an exponential change of $C(t)$. The value of $\tau_{S_3} = 200$ ps obtained from the three-exponential fit to the experimental $C(t)$[73] in the whole time range differs from the time of solvation (about 100 ps) postulated by us. We have made a fit with a three-exponential function in the whole time range at a fixed $\tau_{S_3} = 100$ ps. The other two times (amplitudes) were 3 ps (0.56) and 19 ps (0.35), and the amplitude of the longest component was 0.09 and was almost twice greater than the corresponding value given in Table 3. A decrease in τ_{S_3} caused also a decrease in τ_{S_2} but had no effect on the time and amplitude of the shortest component. The quality of the fit at a fixed $\tau_{S_3} = 100$ ps did not differ much from the that obtained when all parameters were fitted. In Figure 8, both fits would be indistinguishable. So the results of the fit at a fixed τ_{S_3} equal τ_N could also be assumed as correctly describing time changes of $C(t)$.

The interpretation of the spectral and photophysics results, both steady-state and time-resolved, for 4-AP in M-SDS (and for the sake of comparison in the solvents capable of hydrogen-bond formation) given in this work is fully consistent with a description of micelle properties and water molecules comprised in them. Carr et al.[87] have shown for a few probes that M-SDS comprises water molecules forming hydrogen bonds with the probes, and the α and β values determined for these probes are little less than those of bulk water. This evidence confirms that formation of S_1-exc by 4-AP molecules in the S_1-ICT state and water molecules is possible and should be taken into regard in interpretation of results.

Finally, it is worth mentioning that results similar to those obtained by us for 4-AP in M-SDS have been obtained for a few coumarins[51,52] and other molecules containing a donor group (e.g., amino) and an acceptor group (e.g., carbonyl)[88] in protic solvents (alcohols and water). It has been established that in these systems an excited complex (S_1-exc), usually emitting, is formed as a result of formation of a relatively strong hydrogen bond between the carbonyl group of coumarin in the state S_1-ICT and the H−O bond of the molecule of a protic solvent.

5. Conclusions

The main conclusion following from the above analysis is that the classical interpretation of TRES obtained for 4-AP in a micellar environment seems unjustified. As mentioned, the correlation function $C(t)$ can be reliably related to the process of nonspecific solvation only when the shape of TRES does not undergo significant changes with time. The data from Figure 7 clearly indicate that the shape of TRES of 4-AP in M-SDS does change. The full width at half-maximum, Γ, and the asymmetry parameter, γ, increase rapidly to reach a certain constant value. The results imply that the main reason for the changes is the formation of an emitting S_1-exciplex the emission spectrum of which is significantly bathochromically shifted with respect to the 4-AP emission from the S_1-ICT state. This shift is a consequence of formation of a strong hydrogen bond between the carbonyl group of the 4-AP molecule and the H−O bond of the water molecule.

The solvation processes related to the reorientational relaxation of water molecules in micellar systems can be only one of the reasons for the Stokes emission spectra shifts. The normalization of TRES (TRANES) permits a detection of the presence of two species emitting in two different spectral ranges. The results presented prove that such a situation takes place in a system of 4-AP in a M-SDS. The results clearly show that the course of 4-AP deactivation is a complex process. The solvation taking place inside micelles should be treated with caution. Therefore, a proper interpretation of the observed spectral changes requires a deep knowledge of the spectral and photophysical properties of the probe and micellar system studied. Further measurements at a greater time resolution by the TCSPC method or with the up-conversion method, also in other micellar systems, should throw more light on the complex nature of the micellar environment and its effect on the 4-AP deactivation.

Acknowledgment. Dynamics studies were performed at the Centre for Ultrafast Laser Spectroscopy at the A. Mickiewicz University in Poznań. The paper was prepared with the financial

support of KBN (Polish State Committee for Scientific Research) Grant No. 4 T09A 166 24 and Grant No. 4 T09A 119 23.

References and Notes

(1) (a) *Physics of Amphiphiles, Micelles, Vesicle and Microemulsions*; De Giorgio, V., Corti, M., Eds.; North-Holland; Amsterdam, 1985. (b) *Solution Chemistry of Surfactants*; Mittal, K. L., Ed.; Plenum: New York, 1979; Vols. 1 and 2. (c) *Micellization, Solubilization and Microemulsions*; Mittal, K. L., Ed.; Plenum: New York, 1977; Vols. 1 and 2. (d) *Surfactant Solutions New Methods of Investigations*; Zana, R., Ed.; Dekker: New York, 1987.

(2) (a) *Surfactant in Solutions*; Mittal, K. L., Lindman, B., Eds.; Plenum: New York, 1984; Vols. 1 and 2. (b) Kalyanasundaram, K. *Photochemistry in Microheterogeneous Systems*; Academic Press: New York, 1987. (c) *The Chemistry of Excitation at Interfaces*; Thomas, J. K., Ed.; ACS Monograph Series; American Chemical Society: Washington, DC, 1984. (d) Turro, N. J.; Grätzel, M.; Braun, A. M. *Angew. Chem., Int. Ed. Engl.* **1980**, *19*, 675. (e) Bunau, G. V.; Wolf, T. *Adv. Photochem.* **1987**, *14*, 274. (f) *Photochemistry in Organized and Constrained Media*; Ramamurthy, V., Ed.; VCH: New York, 1991. (g) Mallaris, A. *Adv. Colloid Interface Sci.* **1987**, *27*, 153.

(3) (a) Fendler, J. H. *Membrane Mimetic Chemistry*; Wiley-Interscience: New York, 1982. (b) Lindman, B.; Wennerstrom, H.; Eiche, H. F. *Top. Curr. Chem.* **1980**, *87*, 1.

(4) Durchschlag, H.; Tiefenbach, K. J.; Gebauer, S.; Jaenicke, R. *J. Mol. Struct.* **2001**, *563*−*564*, 449.

(5) Bhattacharyya, K.; Bagchi, B. *J. Phys. Chem. A* **2000**, *104*, 10603.

(6) Nandi, N.; Bhattacharyya, K.; Bagchi, B. *Chem. Rev.* **2000**, *100*, 2013.

(7) Vitha, M. F.; Weeckwerth, J. D.; Odland, K.; Dema, V.; Carr, P. W. *J. Phys. Chem.* **1996**, *100*, 18823.

(8) Sarkar, N.; Datta, A.; Swati, D.; Bhattacharyya K. *J. Phys. Chem.* **1996**, *100*, 15483.

(9) Datta, A.; Mandal, D.; Kumar Pal, S.; Das, S.; Bhattacharyya, K. *J. Mol. Liq.* **1998**, *77*, 121.

(10) Kumar Pal, S.; Sukul, D.; Mandal, D.; Sen, S.; Bhattacharyya, K. *Chem. Phys. Lett.* **2000**, *327*, 91.

(11) Hara, K.; Kuwabara, H.; Kajimoto, O. *J. Phys. Chem. A* **2001**, *105*, 7174.

(12) Cho, C. H.; Chung, M.; Lee, J.; Nguyen, T.; Singh, S.; Vedamuthu, M.; Yao, S.; Zhu, J.-B., Robinson, G. W. *J. Phys. Chem.* **1995**, *99*, 7806.

(13) Sarkar, N.; Das, K.; Datta, A.; Das, S.; Bhattacharyya K. *J. Phys. Chem.* **1996**, *100*, 10523.

(14) Das, S.; Datta, A.; Bhattacharyya, K. *J. Phys. Chem. A* **1997**, *101*, 3299.

(15) Datta, A.; Mandal, D.; Kumar Pal, S.; Bhattacharyya, K. *J. Phys. Chem. B* **1997**, *101*, 10221.

(16) Mandal, D.; Datta, A.; Kumar Pal, S.; Bhattacharyya, K. *J. Phys. Chem. B* **1998**, *102*, 9070.

(17) Willard, D. M.; Riter, R. E.; Levinger, N. E. *J. Am. Chem. Soc.* **1998**, *120*, 4151.

(18) Riter, R. E.; Willard, D. M.; Levinger, N. E. *J. Phys. Chem. B* **1998**, *102*, 2705.

(19) Riter, R. E.; Undiks, E. P.; Levinger, N. E. *J. Am. Chem. Soc.* **1998**, *120*, 6062.

(20) Faeder, J.; Ladanyi, B. M *J. Phys. Chem. B* **2001**, *105*, 11148.

(21) Pant, D.; Levinger, N. E. *Langmuir* **2000**, *16*, 10123.

(22) Soujanya, T.; Krishna, T. S. R.; Samanta, A. *J. Phys. Chem.* **1992**, *96*, 8544.

(23) Soujanya, T.; Krishna, T. S. R.; Samanta, A. *J. Photochem. Photobiol.* **1992**, *66*, 185.

(24) Vajda, S.; Jimenez, R.; Rosenthal, S. J.; Fidler, V.; Fleming, G. R.; Castner, E. W., Jr. *J. Chem. Soc., Faraday Trans.* **1995**, *91*, 867.

(25) Datta, A.; Das, S.; Mandal, D.; Kumar Pal, S.; Bhattacharyya, K. *Langmuir* **1997**, *13*, 6922.

(26) Maiti, N. C.; Krishna, M. M. G.; Britto, P. J.; Periasamy, N. *J. Phys. Chem. B* **1997**, *101*, 11051.

(27) Sen, S.; Sukul, D.; Dutta, P.; Bhattacharyya, K. *J. Phys. Chem. A* **2001**, *105*, 7495.

(28) Tada, E. B.; Novaki, L. P.; El Seoud, O. A. *Langmuir* **2001**, *17*, 652.

(29) Bogusz, S.; Venable, R. M.; Pastor, R. W. *J. Phys. Chem. B* **2001**, *105*, 8312.

(30) (a) Matizinger, S.; Hussey, D. M.; Fayer, M. D. *J. Phys. Chem. B* **1998**, *102*, 7216. (b) Cang, H.; Brace, D. D.; Fayer, M. D. *J. Phys. Chem. B* **2001**, *105*, 10007. (c) Kowalczyk, A. A.; Vecer, J.; Hodgson, B. W.; Keene, J. P.; Dale, R. E. *Langmuir* **1996**, *12*, 4358. (d) Mohtat, N.; Cozens, F. L.; Scaiano, J. C. *J. Phys. Chem. B* **1998**, *102*, 7557.

(31) Laguitton-Pasquier, H.; Pansu, R.; Chauvet, J.-P.; Pernot, P.; Collet, A.; Faure, J. *Langmuir* **1997**, *13*, 1907.

(32) Grieser, F.; Drummond, C. J. *J. Phys. Chem.* **1988**, *92*, 5580.

(33) Karmakar, R.; Samanta, A. *J. Am. Chem. Soc.* **2001**, *123*, 3809.

(34) Saroja, G.; Ramachandram, B.; Saha, S.; Samanta, A. *J. Phys. Chem.* **1999**, *103*, 2906.

(35) Ware, W. R.; Lee, S. K.; Brant, G. J.; Chow, P. P. *J. Chem. Phys.* **1971**, *11*, 4729.

(36) Nagarajan, V.; Brearley, A. M.; Kang, T.-J.; Barbara, P. F. *J. Chem. Phys.* **1987**, *86*, 3183.

(37) Harju, T. O.; Huizer, A. H.; Varma, C. A. G. O. *Acta Chem. Scand.* **1995**, *49*, 829.

(38) Soujanya, T.; Fessenden, R. W.; Samanta, A. *J. Phys. Chem.* **1996**, *100*, 3507.

(39) Sen, S.; Sukul, D.; Dutta, P.; Bhattacharyya, K. *J. Phys. Chem. A* **2001**, *105*, 10635.

(40) Wetzler, D. E.; Chesta, C.; Fernandez-Prini, R.; Aramendia, P. F. *J. Phys. Chem. A* **2002**, *106*, 2390.

(41) Harju, T. O.; Huizer, A. H.; Varma, C. A. G. O *Chem. Phys.* **1995**, *200*, 215.

(42) Suppan, P. *J. Chem. Soc., Faraday Trans. 1* **1987**, *83*, 495.

(43) Maroncelli, M.; Fleming, G. R. *J. Chem. Phys.* **1987**, *86*, 6221.

(44) Saroja, G.; Samanta, A *J. Chem. Soc., Faraday Trans.* **1996**, *92*, 2697.

(45) Noukakis, D.; Suppan, P. *J. Lumin.* **1991**, *47*, 285.

(46) Saroja, G.; Samanta, A. *J. Chem. Soc., Faraday Trans.* **1998**, *94*, 3141.

(47) Saroja, G.; Samanta, A. *Chem. Phys. Lett.* **1995**, *246*, 506.

(48) Koti, A. S. R.; Krishna, M. M. G.; Periasamy, N. *J. Phys. Chem A* **2001**, *105*, 1767.

(49) Koti, A. S. R.; Periasamy, N. *Proc. Indian Acad. Sci. (Chem. Sci.)* **2001**, *113*, 157.

(50) M-SDS−water solution of SDS for concentration of SDS above critical micellar concentration ($>8 \times 10^{-3}$ M).

(51) (a) Kapturkiewicz, A.; Herbich, J.; Karpiuk, J.; Nowacki, J. *J. Phys. Chem. A* **1997**, *101*, 2332. (b) Morlet-Savary, F.; Ley, C.; Jacques, P.; Fouassier, J. P. *J. Phys. Chem. A* **2001**, *105*, 11026. (c) Yatsuhashi, T.; Nakajima, Y.; Shimada, T.; Tachibana, H.; Inoue, H. *J. Phys. Chem. A* **1998**, *102*, 8657. (d) Nad, S.; Pal, H. *J. Phys. Chem. A* **2001**, *105*, 1097. (e) Kovalenko, S. A.; Schanz, R.; Farztdinov, V. M.; Hennig, H.; Ernsting, N. P. *Chem. Phys. Lett.* **2000**, *323*, 312.

(52) (a) Nibbering, E. T. J.; Tschirschwitz, C.; Chudoba, C.; Elsaesser, T. *J. Phys. Chem. A* **2000**, *104*, 4236. (b) Tschirschwitz, F.; Nibbering, E. T. *Chem. Phys. Lett.* **1999**, *312*, 169. (c) Chudoba, C.; Nibbering, E. T. J.; Elsaesser, T. *J. Phys. Chem. A* **1999**, *103*, 5625. (d) Lopez Arbeloa, T.; Lopez Arbeloa, F.; Tapia, M. J.; Lopez Arbeloa, I. *J. Phys. Chem.* **1993**, *97*, 4704. (e) Królicki, R.; Jarzęba, W.; Mostafavi, M.; Lampre, I. *J. Phys. Chem. A* **2002**, *106*, 1708. (f) Yip, R. W.; Wen, Y. X. *Can. J. Chem.* **1991**, *69*, 1413.

(53) Karolczak, J.; Komar, D.; Kubicki, J.; Szymański, M.; Wróżowa, T.; Maciejewski, A. *Bull. Pol. Acad. Sci., Chem.* **1999**, *47*, 4.

(54) (a) Press, W. H.; Teukolsky, S. A.; Vetterling, W. T.; Flannery, B. P. *Numerical Recipes in C*; Cambridge University Press: Cambridge, U.K., 1992. (b) Marquardt, D. W. *J. Soc. Ind. Appl. Math.* **1963**, *11*, 341.

(55) (a) Nelder, J. A.; Mead, R. *Comput. J.* **1965**, *7*, 308. (b) Walters, F. H.; Parker, L. R., Jr. *Sequential Simplex Optimization*; CRC Press LLC: 1992.

(56) Karolczak, J.; Komar, D.; Kubicki, J.; Wróżowa, T.; Dobek, K.; Ciesielska, B.; Maciejewski, A. *Chem. Phys. Lett.* **2001**, *344*, 154.

(57) Van den Zegel, M.; Boens, N.; Daems, D.; De Schryver, F. C. *Chem. Phys.* **1986**, *101*, 311.

(58) (a) Saari, P.; Aaviksoo, J.; Freiberg, A.; Timpmann, K. *Opt. Commun.* **1981**, *39*, 94. (b) Schiller, N. H.; Alfano, R. P. *Opt. Commun.* **1980**, *35*, 451. (c) Imhof, R. E.; Birch, D. J. *Opt. Commun.* **1982**, *42*, 83.

(59) Horng, M. L.; Gardecki, J. A.; Papazyan, A.; Maroncelii, M. *J. Phys. Chem.* **1995**, *99*, 17311.

(60) (a) Visser, A. J. W. G.; Kulinski, T.; van Hoek, A. *J. Mol. Struct.* **1988**, *175*, 111. (b) User's manual for TAC Tennelec model TC 864 and for CFD Tennelec model TC 454.

(61) Krystkowiak, E.; Dobek, K.; Kubicki, J.; Maciejewski, A., manuscript in preparation.

(62) Suppan, P.; Ghoneim, N. *Solvatochromism*; The Royal Society of Chemistry, Information Services: 1997.

(63) The parameter α is a measure of hydrogen-bond energy formed by the H−X bonds of the solvent molecule, while the parameter β is a measure of energy of hydrogen bonds formed by lone electron pairs of heteroatoms of solvent molecule. (a) Kamlet, M. J.; Abboud, J. L. M.; Abraham, M. H.; Taft, R. W. *J. Org. Chem.* **1983**, *48*, 2877. (b) Abraham, M. H. *Chem. Soc. Rev.* **1993**, 73. (c) Marcus, J. *The Properties of Solvents*; Wiley: Chichester, U.K., 1998.

(64) (a) Yatsuhashi, T.; Inoue, H *J. Phys. Chem. A* **1997**, *101*, 8166. (b) Simon, J. D. *J. Phys. Chem.* **1991**, *95*, 8466. (c) Morimoto, A.; Yatsuhashi, T.; Shimada, T.; Kumazaki, S.; Yoshihara, K.; Inoue, H. *J. Phys. Chem. A* **2001**, *105*, 8840.

(65) The reason for the differences in the maxima positions of the fluorescence spectra obtained by different authors is not known. The correction curve for our monochromator/photomultiplier was supplied by the manufacturer (Edinburgh Instruments) using a lamp of well-known spectral characteristics. Additionally, the experimentally obtained corrected steady-state emission spectrum of quinine sulfate in 0.1 N H_2SO_4 recorded at the excitation $\lambda_{exc} = 364$ nm was compared with the spectrum given in the literature (Lakowicz, J. R. *Principles of Fluorescence Spectroscopy*, 2nd ed.; Kluwer Academic/Plenum Publishers: New York, 1999; pp 640−641) as a standard and that measured independently by using a calibrated spectrofluorimeter Spex Fluorolog-3-11 (sincere thanks to Dr. E. Sikorska for performance of this measurement) reaching a good agreement in the range $\lambda_{em} < 600$ nm. Moreover, the emission spectra measured by us on independent spectrofluorimeters with independently determined correction curves are in agreement. Perhaps the results reported by different groups were made at different temperature, which could affect (at least partly) the position of the emission spectra maxima.[45] Our results were obtained at 20 ± 1 °C.

(66) Meech, S. R.; Phillips, D. *J. Photochem.* **1983**, *23*, 193.

(67) Ware, W. R. In *Photochemistry in Organized and Constained Media*; Ramamurthly, V., Ed.; VCH Publisher Inc.: New York, 1991; p 563 and references therein.

(68) Bales, B. L.; Messina, L.; Vidal, A.; Peric, M.; Nascimento, O. R. *J. Phys. Chem. B* **1998**, *102*, 10347.

(69) (a) Laermer, F.; Elsaesser, T.; Kaiser, W. *Chem. Phys. Lett.* **1989**, *156*, 381. (b) Mokhtari, A.; Cheriba, J.; Chesnoy, J. *J. Opt. Soc. Am. B* **1990**, *7*, 1551. (c) Kang, T. J.; Ohta, K.; Tominaga, K.; Yoshihara, Y. *Chem. Phys. Lett.* **1998**, *287*, 29. (d) Tan, X.; Gustafson, L.; Lefumeux, C.; Burdziński, G.; Buntix, G.; Poizat, O. *J. Phys. Chem. A* **2002**, *106*, 3593. (e) Kovalenko, A. A.; Schanz, R.; Henning, H.; Ernsting, N. P. *J. Chem. Phys.* **2001**, *115*, 3256.

(70) (a) Nienhuys, H. K. *Femtosecond mid-infrared Spectroscopy of Water*; Technol. University: Utrecht, 2002 and references therein. (b) Laenen, R.; Rauscher, C.; Lauberen, A. *J. Phys. Chem. B* **1998**, *102*, 9304. (c) Cheng, H.-P. *J. Phys. Chem. A* **1998**, *102*, 6201. (d) Gale, G. M.; Gallot, G.; Hache, F.; Lascoux, N.; Bratos, S.; Leicknam, J.-Cl. *Phys. Rev. Lett* **1999**, *82*, 1068. (e) Bagno, A.; Scorrano, G. *Acc. Chem. Res.* **2000**, *33*, 609.

(71) Siano, D. B.; Metzler, D. E. *J. Chem. Phys.* **1969**, *51*, 1856.

(72) Significantly different shapes of TRES obtained for the two times per channel in short times after excitation, and in particular for $t = 0$, illustrate that not only fwhm of IRF but also time per channel adjusted to the dynamics of the processes are important for getting reliable results and their correct interpretation.

(73) The choice of ν^{g}_{em} is probably the best because in the theoretical description of the dynamic, Stokes shift is considered in terms of average solvation energies. So in this paper, $C(t)$ will be analyzed mainly for ν^{g}_{em} and for the least time per channel value.

(74) Huang, Y.; Cheng, T.; Li, F.; Haung, C.-H.; Wang, S.; Huang, W.; Gong, Q *J. Phys. Chem. B* **2002**, *106*, 10041.

(75) The value of $\Delta\nu^{shift}_{em}$(H-bond) is determined from the relation $\Delta\nu^{shift}_{em}$(H-bond) = $\nu^{max}_{em}(f(\epsilon,n)) - \nu^{max}_{em}$(H-bond), where ν^{max}_{em}(H-bond) is the position of maximum of steady-state fluorescence spectrum for 4-AP in a solvent capable of forming a hydrogen bond and $\nu^{max}_{em}(f(\epsilon,n))$ is the position of maximum of steady-state fluorescence spectrum for 4-AP in selected ethers, esters, and nitriles. The solvents should have values of polarity function as similar as possible.

(76) (a) Streletzky, K.; Phillies, G. D. *Langmuir* **1995**, *11*, 42. (b) Vass, Sz.; Gilanyi, T.; Borbley, S. *J. Phys. Chem. B* **2000**, *104*, 2073. (c) Vass, Sz. *J. Phys. Chem. B* **2001**, *105*, 455.

(77) Melo, C. C. E.; Costa, M. B. S.; Maçanita, A. L.; Santos, H. *J. Colloid Interface Sci.* **1991**, *141*, 439.

(78) (a) Bales, B. L.; Howe, A. M.; Pitt, A. R.; Roe, J. A.; Griffiths, P. C. *J. Phys. Chem. B* **2000**, *104*, 264. (b) Bales, B. L.; Szahin, A.; Lindbad, C.; Almgren, M. *J. Phys. Chem. B* **2000**, *104*, 256.

(79) Menger, F. M. *Acc. Chem. Res.* **1979**, *12*, 111.

(80) Yuan, D.; Brown, R. G. *J. Phys. Chem. A* **1997**, *101*, 3461.

(81) Alexion, M. S.; Tychopoulos, V.; Ghorbanian, S.; Tyman, J. H. P.; Brown, R. G., Brittain, P. I. *J. Chem. Soc., Perkin Trans.* **1990**, *2*, 837.

(82) (a) Bhattacharyya, K. In *Organic Molecular Photochemistry*; Ramamurthy, V., Schanze, K, S., Eds.; Marcel Dekker: New York, Basel, 1999; p 283. (b) Chen, Y.; Topp, M. R. *Chem. Phys.* **2002**, *283*, 249.

(83) The value of $\Delta\nu^{shift}_{ab}$(H-bond) is determined like the value $\Delta\nu^{shift}_{em}$(H-bond), but it describes the influence of the hydrogen bonds on absorption spectra position (see ref 75).

(84) It cannot be excluded that apart from S_1-exc there are other emitting complexes in M-SDS, formed as a result of formation of a relatively strong hydrogen bond between the S═O groups of the surfactant molecule and the N−H bonds of the amino group of 4-AP. This supposition arises from the inconsistencies between the TRES spectra obtained from emission decay measurements (for all times after excitation) and the spectra calculated from the steady-state emission of 4-AP in the S_1-ICT state (measured in ACN, where S_1-exc is not formed) and the S_1-exc emission spectrum measured in H_2O, when the contribution of S_1-exc in the total emission is the greatest. The presence of complexes of different stoichiometry for 4-AP in binary solvents has been postulated in ref 40.

(85) Bhattacharyya, K.; Bagchi, B *J. Phys. Chem. A* **2000**, *104*, 10603.

(86) Gustavsson, T.; Cassara, L.; Gulbinas, V.; Gurzadyan, G.; Mialocq, J.-C.; Pommeret, S.; Sorgius, M.; Van der Meulen, P. *J. Phys. Chem. A* **1998**, *102*, 4229.

(87) Vitha, M. F.; Weckwerth, J. D.; Odland, K.; Dema, V.; Carr, P. W. *J. Phys. Chem.* **1996**, *100*, 18823.

(88) (a) Miyasaka, H.; Tabata, A.; Ojima, S.; Ikeda, N.; Mataga, N. *J. Phys. Chem.* **1993**, *97*, 8222. (b) Cramer, L. E.; Spears, K. G. *J. Am. Chem. Soc.* **1978**, *100*, 223. (c) Mataga, N.; Tsuno, S. *J. Chem. Phys.* **1957**, *30*, 711.